ADVANCES IN MATERIALS SCIENCE, Vol. 22, No. 4 (74), December 2022

DOI: 10.2478/adms-2022-0015

Mohamed Ikhlef Chaouch[1]*, Abdelghani Baltach[1,2], Ali Benhamena[1]

[1] *Laboratory LPQ3M, BP763, University of Mascara, Mascara 29000, Algeria*
[2] *Department of Mechanical Engineering, University of Tiaret, Algeria*

* ikhlef.mohamed@univ-mascara.dz

NUMERICAL ANALYSIS OF GEOMETRICAL PARAMETERS EFFECT ON CONTACT ZONE UNDER FRETTING FATIGUE LOADING

ABSTRACT

The fatigue process under fretting conditions is characterized by small oscillatory movements due to vibrating or cyclic loads between two surfaces in contact. Two phenomena can arise as a consequence: the surface wear of the bodies in contact, giving rise to the so-called fretting wear. The second phenomenon concerns crack nucleation in the contact region, causing a reduction in the fatigue strength of the component subjected to cyclic loading. This process is called “fretting fatigue”. In the present study, finite element models (2D-FEM) are provided to demonstrate the effect of pad radius on the contact parameters such as: contact pressure, shear traction, stresses, sliding, size of contact line and crack nucleation and its location along the contact line of aeronautical Al2024 alloy under fretting fatigue loading. Six numerical models are utilized to describe the effect of changing pad radii on contact stresses and damage of crack nucleation. The Ruiz parameter criterion should be used to predict the location of crack initiation in the contact zone. Comparison of the finite element results shows that there is a good agreement between the numerical modeling predictions with those analytical results. The stress field, relative slip, and damage parameters in fretting fatigue loading were highlighted. The pad radius substantially affects the distribution of contact parameters. Particular attention must be taken into consideration to this variable when analyzing the structure in fretting fatigue.

Keywords*: Fretting fatigue; FE model; crack initiation; Ruiz parameter*

INTRODUCTION

Fatigue can be defined as the continuous degradation process of a material when it is subjected to dynamic loads that can cause an accumulation of damage to the material, even if the loads imposed are lower than its yield strength. Fretting fatigue is a special case of fatigue. The fatigue process under fretting conditions is characterized by the relative motion of low amplitude (on the order of microns) between two surfaces in contact induced by vibrating loads or cyclic loads [1]. Among other degradation processes, this slip tends to cause surface wear that can lead to the premature appearance of micro-cracks in the contact region [2,3]. A further examination of the subject of fretting fatigue in various applications can be found in refs [4–6]. Vázquez et al. [7] carried out a series of tests and an analytical and numerical analysis to study the fretting fatigue behavior of the Al7075-T651 alloy. These authors predict the lifetime and crack growth path of this material under fretting fatigue loading of constant

amplitude based on the joint application of the multiaxial fatigue criterion and critical distance methodology. They have concluded that the initiation of cracks in fretting fatigue and its growth are perpendicular to the contact surface in the first step, and then they turn towards the contact zone with an inclination angle equal to about 3°. It seems that this approach gives better results in terms of crack growth in the contact zone. Luke et al. [8] investigated the fretting fatigue behavior of EA4T (25CrMo4) material, and they concluded that the fatigue life of railway axles can be limited by crack initiation in press fitting locations, in particular within the contact zone between the axle and the wheel. They also revealed that the use of the multiaxial fatigue parameters provides a consistent correlation with the fretting fatigue crack initiation for different specimen types and loading conditions and may be potentially considered in the fatigue assessment of full-scale axles. Pinto et al. [9] developed a numerical model to study the effect of sequences of variable amplitude shear loading on the level of contact tractions/stresses of Al 7075-T651 alloy under fretting fatigue loading. These authors investigated the fretting fatigue behavior of this material using the multiaxial fatigue criterion and cumulative damage model, again, they found, that the proposed life estimation procedure was enhanced to include the effect of material loss due to wear. In contacts under fretting, there are basically two situations identified, which are partial and total slip. The analytical model for the stresses in the fretting contact area was independently proposed by Cattaneo [10] and Mindlin [11]. According to these authors, in fretting fatigue, generally, the applied shear loading is less than the threshold for total slip. Thus, two symmetrical and distinct regions appear within the contact zone: (i) a region of length 2c, known as the stick zone, in which there is no relative tangential movement between the corresponding particles of the bodies in contact; (ii) a peripheral region known as the slip zone, located at the ends of the contact and the stick zone. Recent work by Dhaka et al. [12] adopted a different contact configuration in order to study the effect of the radius of the corners of the contact pad and the length of the flat region on the peak tensile stress under fretting loading. They showed that the peak tensile stress in the fretting direction decreased with an increase in the contact zone. Also, Zhang et al. [13] developed a numerical model to investigate the effect of contact geometry on the frictional behavior of Ti–6Al–4V and showed that the flat geometry can support a stabilized partial slip solution with an associated wear pattern. Chakherlou et al. [14] presented an experimental study and anumerical model in order to simulate the effect of cold expansion of Al-alloy 2024-T3 plates under fretting fatigue. They indicated that the crack nucleation location is in an area away from the hole. Walvekar et al. [15] proposed a damage model for fretting fatigue of AISI4140 vs.Ti-6–4 in a cylinder-on-flat contact configuration, this model replicates the fretting fatigue experiments and estimates the fretting fatigue life of the structure. Vantadori and Zanichelli [16] used the shot peening treatment on the contact surface in order to improve the life of fretting fatigue-affected components. In the same context, the crack growth path in the fretting fatigue specimen repaired by the stop hole method has been carried out by Deng et al. [17]. They have shown a significant impact on the fretting fatigue crack propagation lifetime. Zaleski and Skoczylas [18] investigated experimentally the effects of slide burnishing on the surface roughness, surface layer micro-hardness, and fatigue life of Ti6Al2Mo2Cr titanium alloy parts, who found that the changes in the surface layer properties induced by slide burnishing lead to an increased lifetime of the components. Based on the above, it can be noted that the fretting is a challenging physical phenomenon, which involves different sciences, i.e. tribology, contact mechanics, fatigue, fracture mechanics, corrosion, among others [2]. Other parameters can also affect the fatigue life of structures under fretting fatigue loading. Dobromirski [19] listed more than 50 of them. Today, the question still remains open, and approaches from data science are beginning to be used to study the fretting fatigue behavior of materials. These variables were divided into two

classes, primary and secondary variables, which directly and indirectly affect the fretting-fatigue behavior of any material. In addition, the large number of interacting variables that affect fretting fatigue make experimental testing difficult, and the fretting fatigue of materials is not fully understood and represents a very active research field. These facts led the authors to focus the current investigation on studying the fretting fatigue of Al 2024-T3 alloy under fretting fatigue loading. The main purpose of this work is to find the best way to apply boundary conditions to simulate the fretting fatigue phenomenon using the finite element method. The effects of the loading magnitude, geometrical parameters, stress/strain, pressure, shear traction, sliding, and crack initiation on the contact zone were highlighted.

THEORY AND FORMULATION

Figure 1 depicts a schematic diagram of the contact problem. The normal force is applied to the half-body of the cylinder's top surface, and sliding occurs in the same plane in the horizontal direction. 2a gives the length of the contact area, and R gives the radius of the cylinder. F is the normal force. The pressure distribution and maximum value can be predicted using the Hertz formulation [20]. The following is the contact pressure between the surfaces.

$$a = 2\left(\frac{PR}{\pi E^*}\right)^{1/2} \tag{1}$$

$$E^* = \left(\frac{1-\nu_1^2}{E_1} + \frac{1-\nu_2^2}{E_2}\right)^{-1} \tag{2}$$

$$P_0 = \frac{2P}{\pi a} = \left(\frac{PE^*}{\pi R}\right)^{1/2} \tag{3}$$

$$P(x) = P_0\sqrt{1-\left(\frac{x}{a}\right)^2} \tag{4}$$

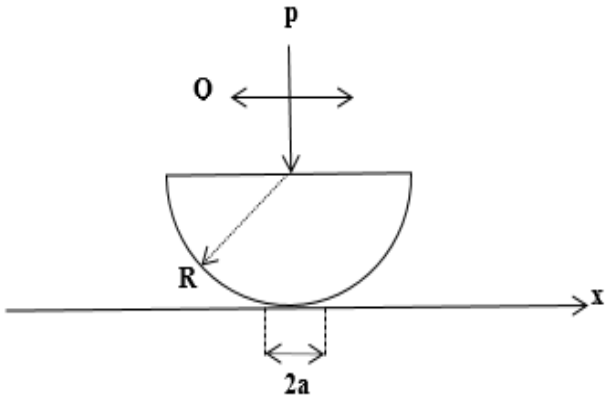


Fig. 1. Schematic of fretting contact problem

P signifies the pressure distribution, while P_0 denotes the maximum pressure distribution that occurs in the contact area's center. The elastic modulus and Poison's ratio are denoted by *E* and *v*, respectively, while shear traction is given by:

$$q(x) = \mu p_0 \sqrt{1 - (\frac{x}{a})^2}, \qquad \text{if} \quad c \le |x| \le a \tag{5}$$

$$q(x) = \mu p_0 \sqrt{1 - (\frac{x}{a})^2} - \mu p_0 \frac{c}{a} \sqrt{1 - \left(\frac{x}{c}\right)^2}, \qquad \text{if} \quad |x| < c \tag{6}$$

There are two types of fretting based on the magnitude of the horizontal load. Both surfaces stick together in the central area of contact ($c \le |x| \le b$) under low horizontal loads. The surfaces slide slowly against each other at both ends of the contact area ($|x| \le c$). This is known as a "partial slip." When the horizontal load is increased, the center of contact area shrinks and the two surfaces slide against each other. This is a "total slip." The friction force distribution on the plane, as seen, has a discontinuity at the boundary of the stick/slip zone at x = ∓ c. This is the most possible location for vacancy accumulation and crack initiation. This means that the stress values at these points determine the fatigue life of components under fretting loads.

When a fatigue stress σ_A is applied, the stick zone will be offset by a distance e, thus creating an asymmetry between the stick and slip zones. The pressure distribution does not change according to Cattaneo [10] and Mindlin [11], the distribution of shear stress under fretting fatigue condition is expressed by the following relationships:

$$q'(x) = \mu p_0 \sqrt{1 - (\frac{x}{a})^2} \qquad \text{If} \quad -a \le |x| \le -c + e \tag{7}$$

$$q'(x) = \mu p_0 \sqrt{1 - (\frac{x}{a})^2} - \mu p_0 \frac{c}{a} \sqrt{1 - \left(\frac{x-e}{c}\right)^2} \quad \text{If} \quad -c + e \le |x| \le c + e \tag{8}$$

$$q'(x) = \mu p_0 \sqrt{1 - (\frac{x}{a})^2} \qquad \text{If} \quad c - e \le |x| \le a \tag{9}$$

$$e = \frac{\sigma_F \, a}{4 \mu p_0} \tag{10}$$

It is known that in fretting fatigue loading, the stress fields in the contact zone are in general complex and non-proportional, so the use of stress-strain based multiaxial models becomes more suitable.

According to Ruiz et al. [21], slip amplitude must be included in the damage parameter to predict crack initiation in fretting fatigue. This author formalized the damage parameter using the maximum shear tension and the local slip amplitude. Based on dovetail experiments, he introduced the first damage parameter.

$$F_1 = \tau . d_x \tag{11}$$

It was discovered that the maximum value of damage parameter F_1 corresponds closely to the location of maximum damage discovered experimentally. It also emphasizes the importance of shear stress as a primary variable in the damage nucleation process. Because a large number of micro cracks can form during fretting fatigue, the maximum damage

nucleation location and the actual crack initiation location may differ. Furthermore, they also observed that the surface damage is converted into a crack due to the presence of tensile stress σ_{xx}. As a result, by multiplying the first damage parameter (F_1) with tensile stress at the same surface location; a new parameter called the initiation parameter F_2 was developed. This parameter is derived from experimental results and is given by:

$$F_2 = \sigma_{xx} \tau d_x \tag{12}$$

NUMERICAL APPROACH

To ensure the life of components affected by fretting fatigue, it is necessary to perform very long and complex tests in the design process. By means of computer models, it is possible to simulate and analyze this component, thus reducing the need to carry out extensive and costly experimental tests and also allowing optimization alternatives. The finite element method is, in general, an interesting numerical analysis technique for this type of analysis. The solution process of the fretting fatigue problem is carried out by the finite element model in the ABAQUS commercial code [22]. In two-dimensional models (plane strain case) for fretting fatigue problems, they can predict results similar to those of three-dimensional models, according to Vázquez et al. [23] and in refs [24,25]. In order to reduce the computational time, only half of the problem was modeled since it is symmetric along the Y axis. The finite element mesh consists of two-dimensional elements with four nodes (CPE4R). There are some special formulations for finite elements that allow the possibility of contact between surfaces to be considered in fretting fatigue analysis. There are two discretization techniques for contact surfaces: Node to Surface and Surface to Surface. In both cases, a master and slave surface must be adopted, which, during the simulation, interact with each other, creating new boundary conditions for the analysis of contact problems. In the contact line, the mesh was built in a structured way, while in the other regions, the use of coarse elements allowed to reduce the level of discretization outside the area of interest in order to reduce the time of calculation (mesh size of 5 μm). The geometrical model and loading conditions are given in Figure 2. The friction coefficient was defined as 0.65. The numerical method for solving nonlinear Newton-Raphson systems is used to solve nonlinear systems of equations. This numerical method is preferable because it has a higher convergence rate for the solution.

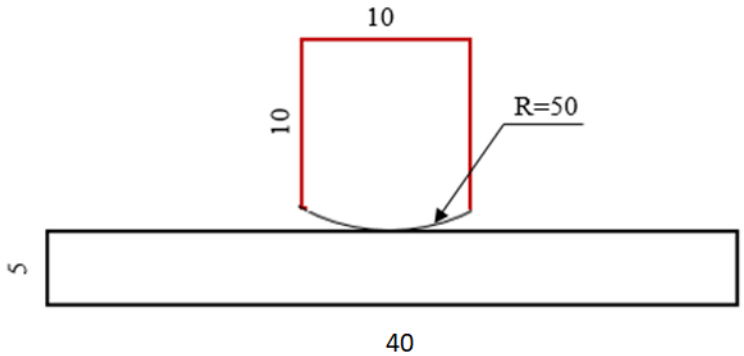


Fig. 2. Geometry of the fretting fatigue model (all dimensions are in mm)

The material of the pad and specimen is an aluminum 2024-T3 alloy. This kind of material is widely used in the aeronautical industry because of its good fatigue and corrosion

characteristics. The specific chemical composition of this material is listed in Tab. 1. The elastic properties at room temperature obtained were: Young's modulus, E = 72100 MPa, Poisson's ratio, ν=0.33.

Table 1. *Chemical composition of the Al2024-T3 [26]*

Al2024-T3	Al	Si	Fe	Cu	Mn	Mg	Cr	Zn	Ti	Others
Max %	Base	0.5	0.5	4.9	0.9	1.8	0.1	0.25	0.15	0.05
Min %				3.8	0.3	1.2				

Abaqus used a pure Master/Slave algorithm. This means that the nodes of the slave surface cannot penetrate the master surface. On the other hand, the master surface can penetrate the slave surface. In general, one will choose as a slave surface the one having the finest mesh or the one forming part of the softest body. Rigid surfaces can only be master surfaces. Two algorithms exist to track the relative motion of surfaces. The finite sliding option is chosen. Normal contact and friction can be modeled by the penalty method or the Lagrange multiplier method. In order to correctly simulate fretting fatigue conditions, the loads were divided into three stages, where each stage constitutes a step of the model. In the first step, the top of the pad was pressed against the specimen surface by a normal load of F=543 N, and this compressed condition was held constant until the end of the cycle. Then, a tangential force of Q = 155 N was applied to the sides of the specimen (the ratio of Q is −1). Finally, in the third loading step, axial stresses were applied to the specimen (σ_A = 100 MPa where (the ratio of σ_A is 0.1). As shown in Figure 3, in the contact region, two partitions were made to improve the mesh refinement.

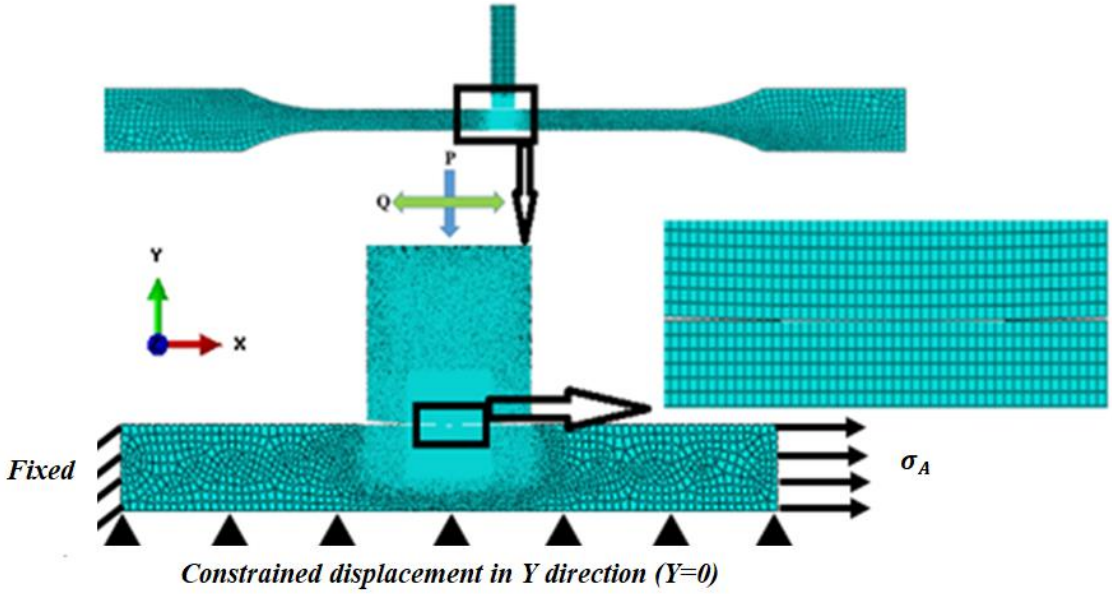


Fig. 3. Finite element detail for the assembled model and loading conditions

The mesh is made with a two-dimensional element with four nodes with an edge size of 5 μm in the contact region. In Figure 4, it is possible to observe how the load conditions vary as the simulation time advances.

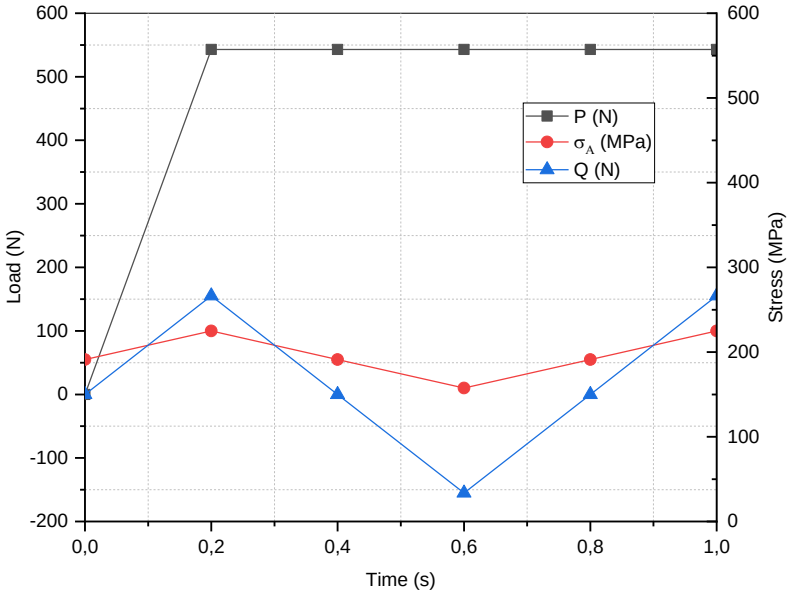


Fig. 4. Simulation of loading condition in fretting fatigue

RESULTS AND DISCUSSION

Validation of the finite element model

The finite element models are verified with the analytical solution using a plane strain analysis. To compute the analytical solution, the reader may refer to [27,28]. A mesh size of 5 μm is used near the contact interface to fulfill the plane strain condition. Figures 5 and 6 depict the comparison between the analytical and the model for contact pressure and shear stress at the contact interface using the literature's data set. These comparisons between the numerical result and the analytical solution of Hills and Nowell [28], where p(x) is the normal contact stress, q(x) is the tangential contact stress.

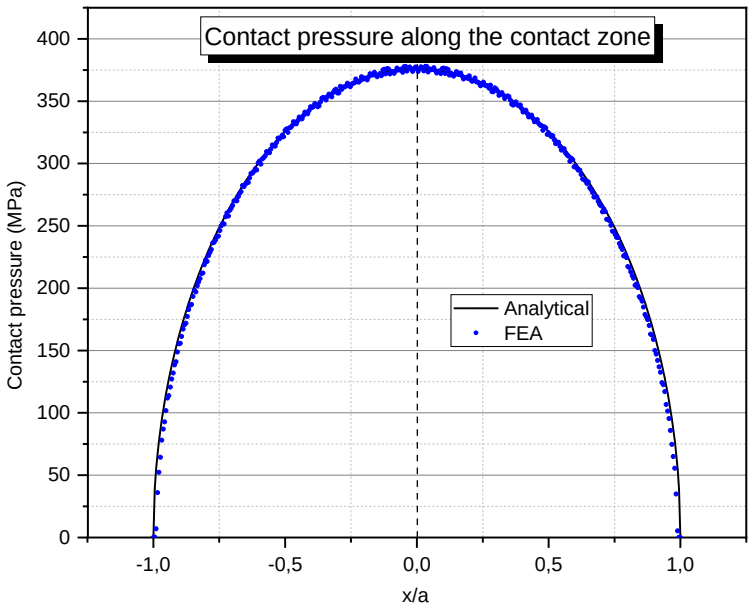


Fig. 5. Comparison of contact pressure along the contact line; numerical and analytical results

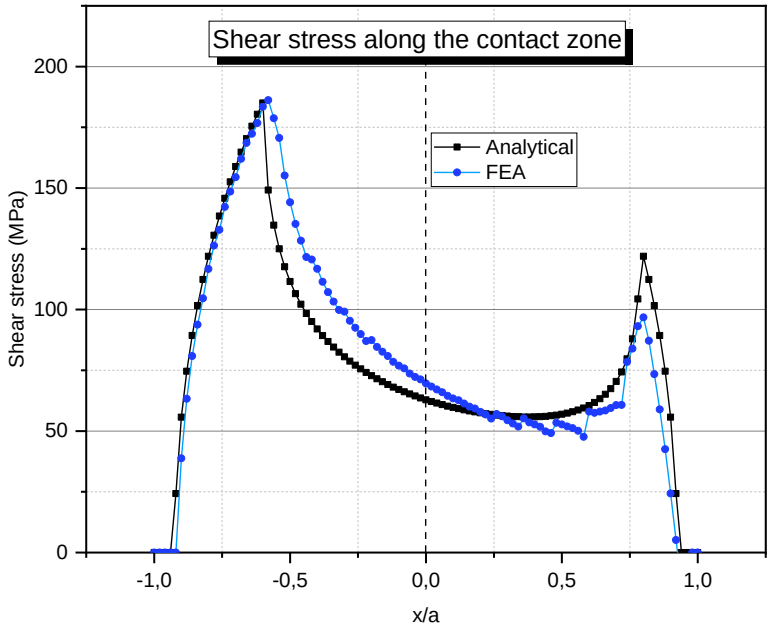


Fig. 6. Comparison of shear stress along the contact line; numerical and analytical results

In general, a good correlation is observed between analytical and finite element solutions (Figures 5 and 6). The percentage error between analytical peak shear traction and finite element solution is less than 5%, and the percentage error in semi-contact width is less than 2% for all the models. The results show agreement in relation to the analytical solution, despite some difference when the tangential stress q(x) reaches its maximum value. It can be noted that different regions correspond to different physical mechanisms that control the process of fretting fatigue. The zone of low shear traction corresponds to the absence of relative sliding of the surfaces in contact (stick zone). In the partial slip zone, which corresponds to the contact state in which the high level of shear traction is observed, fatigue cracks form on the contact areas and, as a result of repeated deformations, wear particles separate. From a practical point of view, the knowledge of the wear mechanism by fretting is interesting to evaluate the service life of a contact connection. The shortest life is expected for connections operating under conditions of transition from partial slip to severe slip. This fact can be explained by the fact that in this range of relative tangential displacements, the formation of wear particles occurs quite intensively, but their removal from the contact zone remains difficult.

Stress analysis

Figure 7 shows the distribution of Von Mises (S_{vm}) stress contours at the contact interface during a fretting cycle for different loading levels.

Figure 7a shows the results of equivalent stress (S_{vm}) at a maximum normal loading level (step 1). Figure 7b-c shows the surface stress in terms of the von Mises stress at the full fretting fatigue cycle, when the horizontal displacement acts on the pad in the correct direction at step 2 (Figure 7b), and finally when the horizontal displacement is acting to the left at step 3 (Figure 7c). This behavior is in accordance with Mindlin [11]; the micro-slip begins at the periphery of the contact. This micro-slip zone can be considered as a ring with an interior radius and an exterior radius. When the bulk stress is applied, there is sliding with friction. On the other hand, the non-slip hypothesis dominates. The sliding surface in fretting

can be broken down into two domains called stick and slip. At the center of the contact, there is a constant so-called stick zone. It is surrounded by a zone where slippage is significant (slip zone). The same conclusions have been found by other authors [3,6].

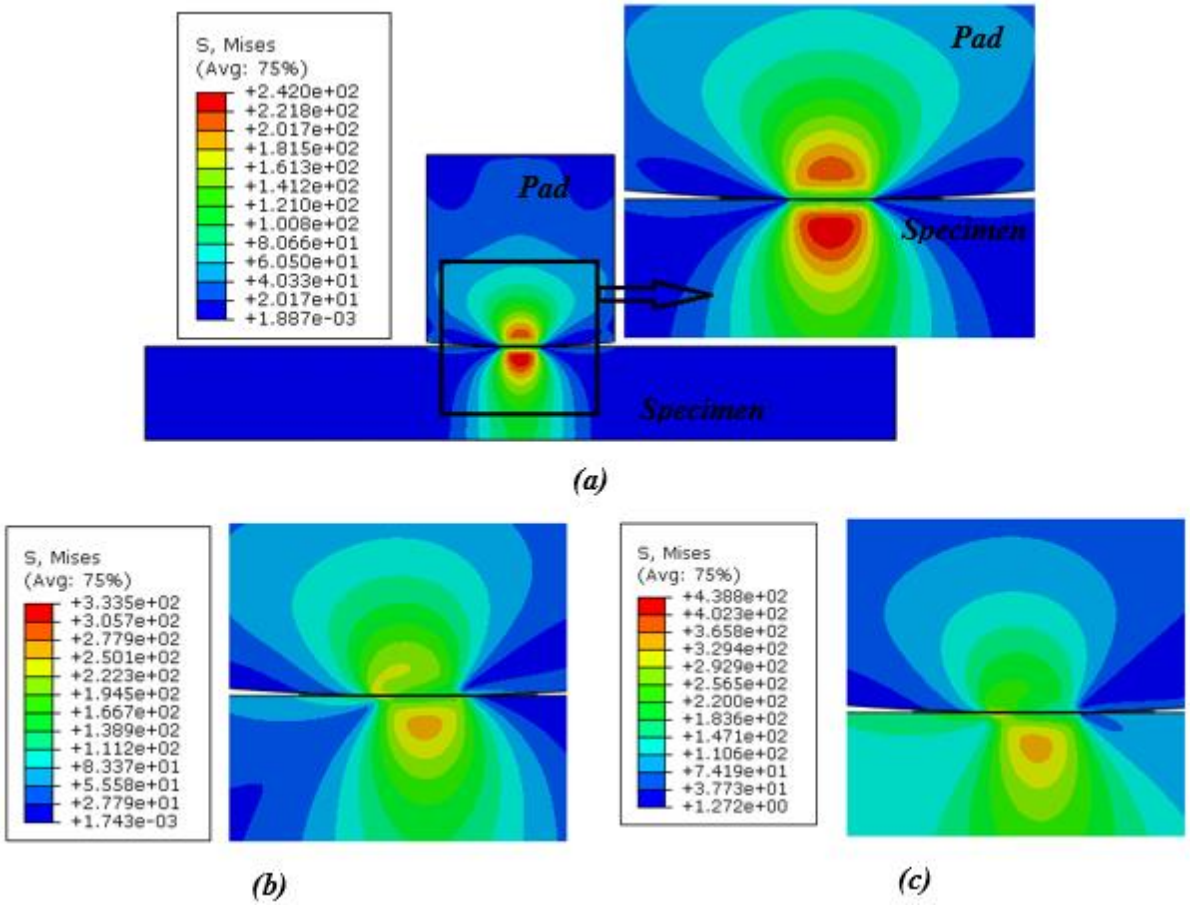


Fig. 7. Distributions of Von Mises stress. a) Step1 (contact hertz). b) The second step (fretting wear) ; and c) step 3 (fretting fatigue)

In service under fretting fatigue loading, it is known that the contact between two surfaces generates multiaxial stresses in the subsurface of the material. This stresses fields, which are responsible for the nucleation of cracks that cause the failure of structures. Figure 8a-c illustrates the different normal and shear stress contours. In Figure 8a, there is a plastic deformation generated by the axial stress (σ_x) at the contact surface, but only a small layer of plastic deformation at a distance from the contact zone. In Figure 8b, the distribution of normal stress (σ_y) shows that the tension stress does not occur due to the high level of contact pressure in this direction. According to Figure 8c, the specimen is under tension and compression stresses in the contact zone. The stress field is important to the contact area, and particularly at the edge of the contact area (σ_{xy}) that requires special attention. This field of stress is concentrated in an inclined plane with respect to the plan of application of the cyclic load. As a result, the high stress gradient in this orientation increases the risk of nucleation and crack growth, which confirms the experimental observation of Vázquez et al. [7].

From Figure 8, it can be noted that the sign of all the stress components in the center of the contact zone is negative. This is obviously due to the effect of the contact pressure, which generates concentrations of compressive stresses at the edge of the contact zone, which can initiate cracks at this location. From the point of view of the phenomenon of concentration in mechanics, the node which corresponds to a position defined by a maximum

constraint along the zone of contact is the most critical position because the component of the stress which sets off the crack initiation and its growth in the specimen has reached its maximum value. This point will be the first to fail if a critical load is reached. These results are very consistent with experimental observations [7,8] where crack initiation occurs in the contact zone. The experimental results show that the fretting under mixed mode loading occurs because the stress field at the contact zone is multiaxial.

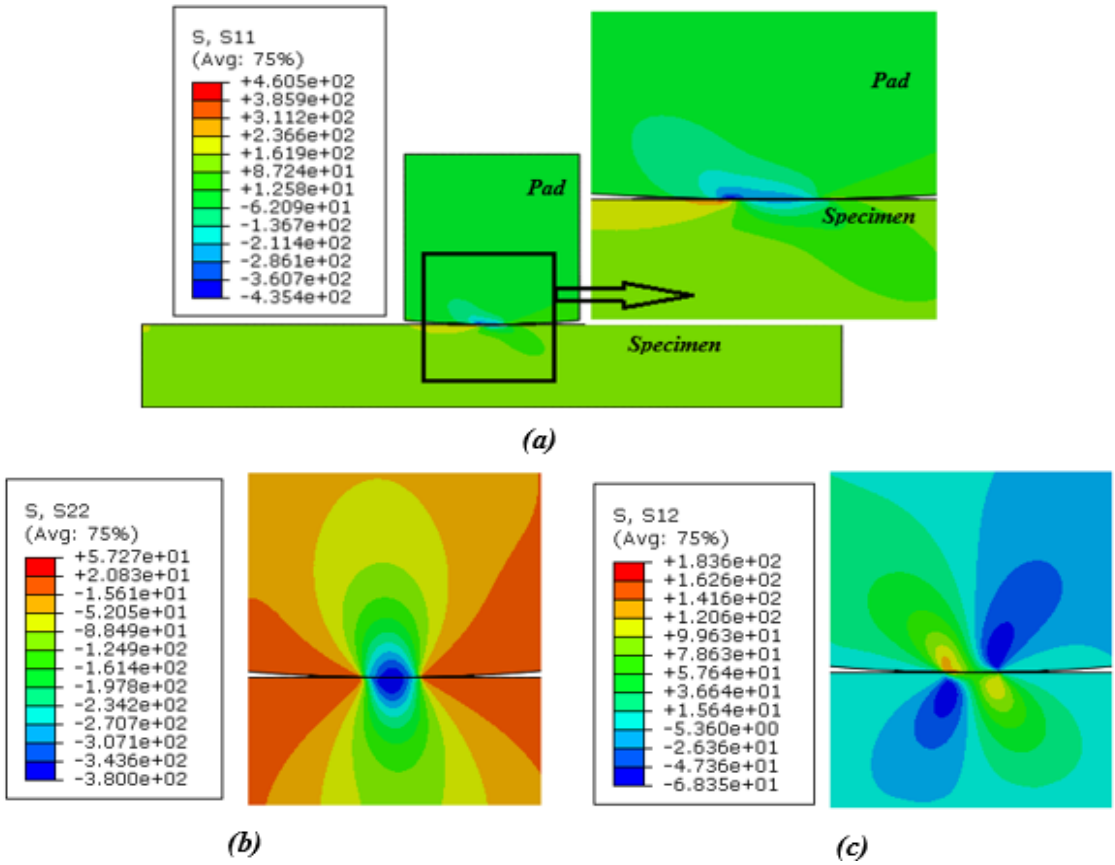


Fig. 8. Stress distribution a) σ_{xx} (S11); b) σ_{yy} (S22) and c) σ_{xy} (S12)

Pad radius effect

The effects of pad radius on the level of contact pressure and shear traction along the contact line are shown in Figures 9 and 10, respectively. Six values of pad radius were taken in the numerical modeling (R = 50, 60, 70, 200, 500 and 1000 mm). These results (Figure 9) show that the shape of any contact pressure or shear stress along the contact line is similar with respect to the size of the pad radius. It can be noted, that the peak of the contact pressure decreases with increasing pad radius whereas the contact width decreases, indicating that the maximum contact pressure is at the minimum contact radius. This behavior may be explained by the fact that the decreasing of the pad radius leads to a narrow line of contact, and consequently, which also leads to a higher stress level at the contact zone. In other words, a transfer of higher contact pressure level from the pad to the specimen through the contact phenomenon, leads to a decrease in specimen stiffness and, consequently, to the failure of the fretting fatigue life of mechanical components in service.

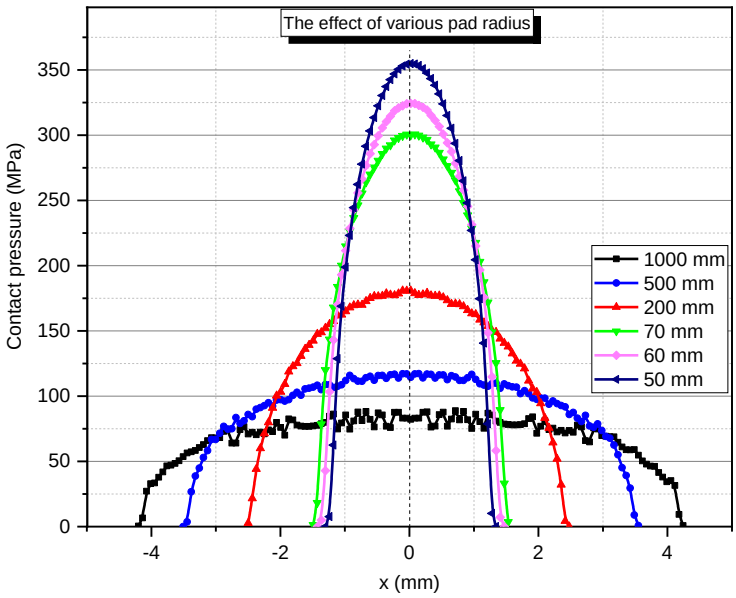


Fig. 9. Evolution of contact pressure under various pads radii

Figure 10 shows the evolution of shear stress q(x) along the contact line at different values of the pad radius mentioned above. It is noticed that the slip zone evolves according to the pad radius while the peak value of the shearing stress decreases. The same conclusion was found previously (Figure 9).

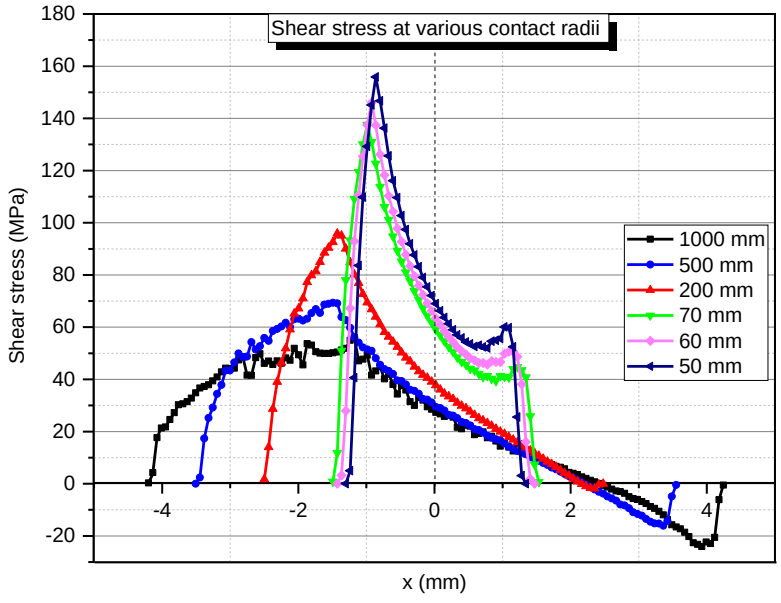


Fig. 10. Evolution of shear stress under various pads radii

Mechanically, a smaller pad radius produces less contact surface as well as higher contact pressures for the same normal loading. This agrees with the previous hypothesis that higher contact pressures cause higher shear stress values and a lower size of contact area. This can be explained by the fact that the lower radius imposes higher contact pressure and shear stress, which reduce the size of the contact zone. The contact shear stresses become zero in the region where contact between the pad and the specimen does not occur, but fretting fatigue

occurs when mechanical components in contact experience relative oscillatory motion between the contact surfaces due to cyclic loading.

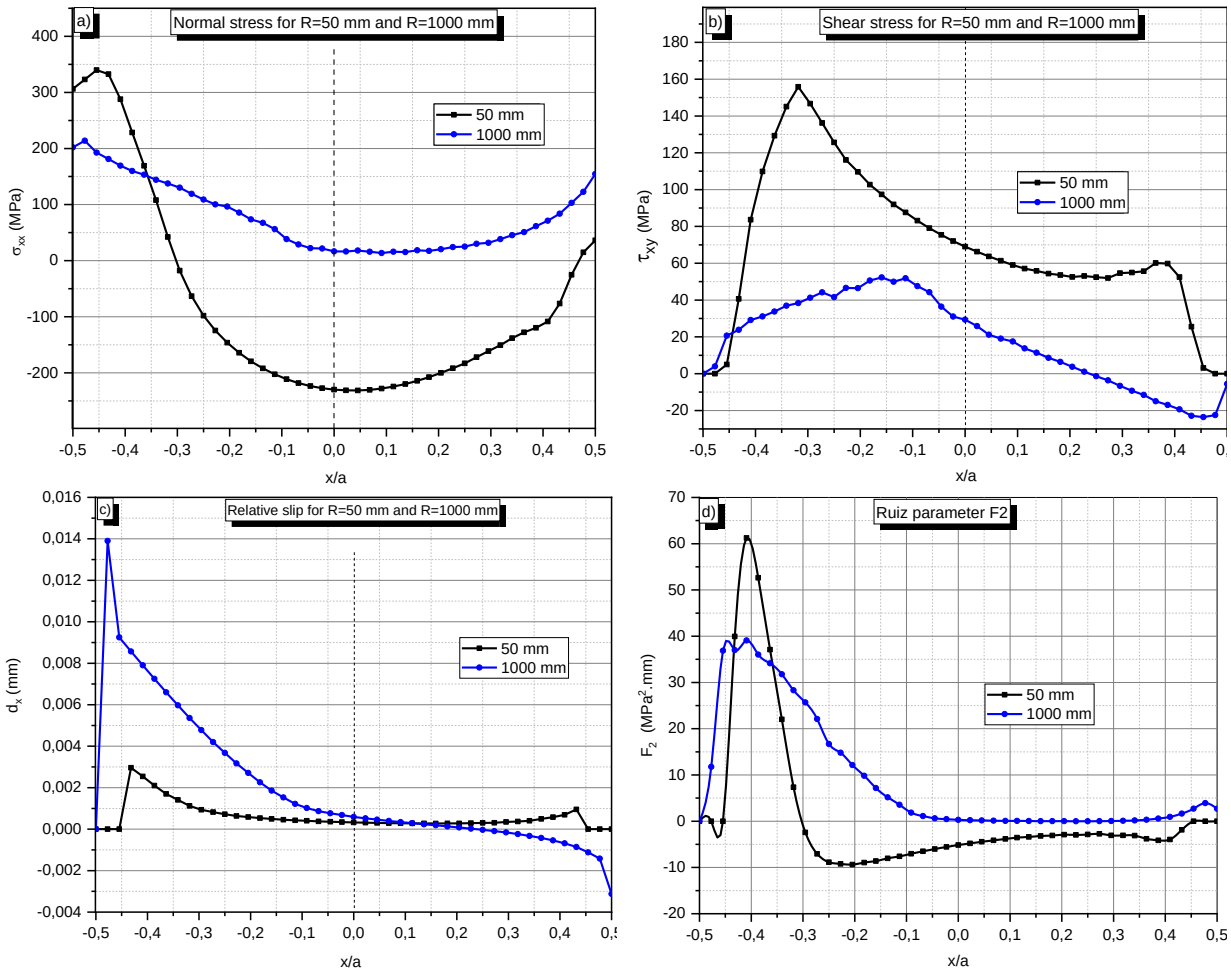


Fig. 11. FE results for R=50 mm and R=1000 mm:a) normal stress; b) shear stress; c) relative slip; and d) Ruiz parameter F2

The application of methodologies to estimate the crack nucleation and its location under fretting fatigue loading is generally based on the determination of the cyclic stress and strain fields in the contact region.

The influence of pad radius on the distribution of stresses along the contact line can be seen in Figures 11a and 11b and its main effect is to increase the level of these components of stress at locations in the contact zone close to the point characterized by x/a = −1. These graphs shown above present the expected profile and are in agreement with what is found in the literature. Figures 11c and 11d show the variation of the slip components and Ruiz parameters along the contact line, note that F2 is maximum at the contact surface. The maximum absolute value of the Ruiz parameter indicates the location of crack nucleation in the contact zone [21]. The peak value of the Ruiz parameter in the case of the pad with R=1000 mm is smaller than the peak value of the pad with R=50 mm, so in this case the crack initiation starts in the model with the smaller pad radius.

The results of the size of the contact line are shown when the pad radius is varied as illustrated in Figure 12, the lower pad radius leads to a decrease in the size of the contact line.

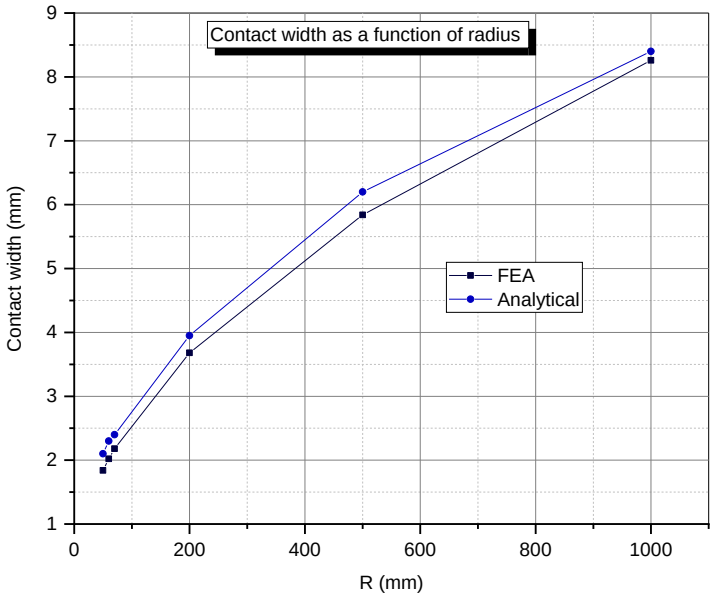


Fig. 12. Comparison of analytical and FEA contact widths as a function of radius

This can be explained by the fact that higher values of pad radius (R) produce lower rated stresses under the contact zone for the same loading condition. On the other hand, for lower pad radii, a maximum contact pressure leads to a reduced size of the contact zone and therefore accelerates the crack nucleation in the contact zone. Similar behaviors are found in other analysis.

Figure 13, in turn, illustrates, for the same material and under the same condition of loading, the effects of varying the pad radius on the peak of contact pressure (Figure 13a). The evolution of peak pressure (P_0) versus pad radius (R) quite an hyperbolic form, which means the increase in pad radius reduces the level of stress in the contact surfaces, which in turn avoids the risk of crack initiation. Figure 13b illustrates, the responses obtained from the finite element modeling terms of the peak of contact pressure versus the size of the contact line. From a qualitative point of view, the evolution presents similar behaviors. The FEA model agrees well with the analytical model with a 2% margin of error.

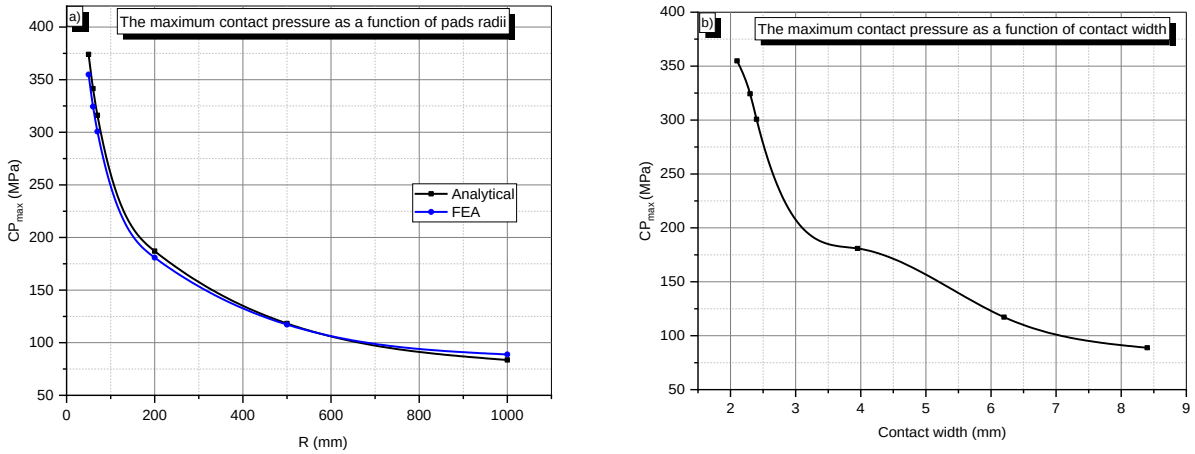


Fig. 13. Evolution of maximal contact pressure as function of: a) pads radii; and b) contact width

It is of great importance to map these variables and understand the effect of pad radius on the peak of contact pressure and on the size of the contact line in fretting fatigue loading.

Firstly, the contact pressure distribution will be evaluated over the entire area of the contact line, considering the following three axes, along the x axis: the pad radius, along the y axis: the size of the contact line; and finally, along the z axis: the peak of contact pressure.

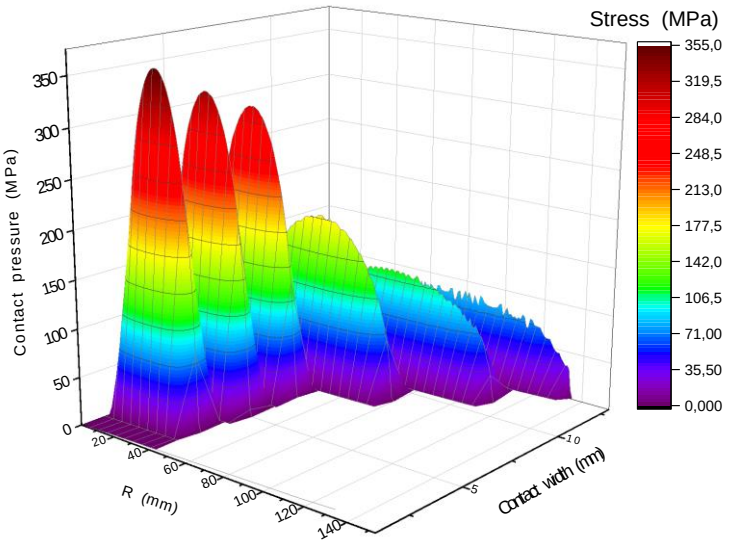


Fig. 14. Stress distribution and contact width in various pads radii

Figure 14 shows the graph of the effect of pad radius on the contact pressure and on the contact line. The level of maximal contact pressure (355 MPa) is localized in the model with the minimum pad radius and the minimum contact width. This means that the model with a smaller pad radius causes stress concentration on a small contact width (less than 2 mm), and that as the pad radius increases, the stress concentration decreases. Therefore, in this case, it can be said that the model with the largest pad radius (1000 mm) has the most suitable pad radius for various models because it has the lowest stress concentration.

CONCLUSIONS

The aim of this study was to validate the present numerical results with the analytical results on the one hand, and to study the effect of pad radius of aeronautical Al2024 alloy on the behavior of contacts in multiaxial fretting fatigue conditions. The effect of pad radius on stress fields, crack nucleation, and its location in the contact zone were predicted using the Ruiz parameter. From these numerical results, we can deduce the following conclusions:

- The development of a finite element modeling approach to simulate the fretting fatigue of materials.
- A good correlation was found between the FEM simulations and the analytical results.
- The peak of contact pressure and the stresses are related to the pad radius.
- Pad radius has a great effect on the size of the contact line and on the crack location of the component under fretting fatigue.
- The change in geometrical parameters has significantly changed the contact stress fields.
- The relative slip across the contact line is related to the level and the distribution of the contact stress fields.

- The relative slip decreases significantly with the decreasing of pad radius.
- The maximum stress field is located at the stick-slip interface along the contact line.
- Apply the Ruiz parameter in fretting fatigue to estimate crack nucleation along the contact zone.
- In this study, the crack initiation starts in the model with the smaller pad radius.

REFERENCES

1. Vingsbo, O., Söderberg, S. On fretting maps. Wear 126 (1988) 131-147.
2. Abbasi, F., Majzoobi, G. H., Mendiguren, J. A review of the effects of cyclic contact loading on fretting fatigue behavior. Advances in Mechanical Engineering 12 (2020) 1687814020957175.
3. Benhamena, A., Talha, A., Benseddiq, N., Amrouche, A., Mesmacque, G., Benguediab, M. Effect of clamping force on fretting fatigue behaviour of bolted assemblies: Case of couple steel–aluminium. Materials Science and Engineering: A 527 (2010) 6413-6421.
4. Gu, H., Jiao, L., Yan, P., Ma, B., Chen, S., Feng, L., Wang, X. Crack behavior of Ti-6Al-4V alloy combined conformal contact fretting, non-conformal contact fretting and simple fatigue. International Journal of Fatigue 139 (2020) 105741.
5. Hamadouche, F., Benzaama, H., Mokhtari, M., Tahar, M. A. Influence of contact parameters in fretting-fatigue contact 3D problems. Frattura ed Integrità Strutturale 15 (2021) 228-240.
6. Benhamena, A., Amrouche, A., Talha, A.,Benseddiq, N. Effect of contact forces on fretting fatigue behavior of bolted plates: Numerical and experimental analysis. Tribology International 48 (2012) 237-245.
7. Vázquez, J., Carpinteri, A., Bohórquez, L., Vantadori, S. Fretting fatigue investigation on Al 7075-T651 alloy: Experimental, analytical and numerical analysis. Tribology International 135 (2019) 478-487.
8. Luke, M., Burdack, M., Moroz, S., Varfolomeev, I. Experimental and numerical study on crack initiation under fretting fatigue loading. International Journal of Fatigue 86 (2016) 24-33.
9. Pinto, A. L., Cardoso, R. A., Talemi, R., Araújo, J. A. Fretting fatigue under variable amplitude loading considering partial and gross slip regimes: Numerical analysis. Tribology International 146 (2020) 106199.
10. Cattaneo, C. Sul contatto de due corpielastici: Distribuzione locale deglisforzi. Rendicontidel l'Accademianazionale dei Lincei 6 (1938) 342-349.
11. Mindlin, R. D. Compliance of elastic bodies in contact. ASME Journal of Applied Mechanics 16 (1949) 259–268.
12. Dhaka, P., Prakash, R. V. Effect of Contact Geometry on the Contact Stresses in a Flat with Round Edge Contact. Frattura ed Integrità Strutturale 13 (2019) 630-638.
13. Zhang, T., McHugh, P. E., Leen, S. B. Computational study on the effect of contact geometry on fretting behaviour. Wear 271 (2011) 1462-1480.
14. Chakherlou, T. N., Shahriary, P., Akbari, A. Experimental and numerical investigation on the fretting fatigue behavior of cold expanded Al-alloy 2024-T3 plates. Engineering Failure Analysis 123 (2021) 105324.
15. Walvekar, A. A., Leonard, B. D., Sadeghi, F., Jalalahmadi, B., Bolander, N. An experimental study and fatigue damage model for fretting fatigue. Tribology International 79 (2014) 183-196.

16. Vantadori, S., Zanichelli, A. Fretting-fatigue analysis of shot-peened aluminium and titanium test specimens. Fatigue & Fracture of Engineering Materials & Structures 44 (2021) 397-409.
17. Deng, Q., Yin, X., Wang, D., Wahab, M. A. Numerical analysis of crack propagation in fretting fatigue specimen repaired by stop hole method. International Journal of Fatigue 156 (2022) 106640.
18. Zaleski, K, Skoczylas, A. Effect of slide burnishing on the surface layer and fatigue life of titanium alloy parts. Advances in Materials Science 19 (2019) 35-45.
19. Dobromirski, J. M. Variables of fretting process: are there 50 of them? ASTM Special Technical Publication 1159 (1992) 60-60.
20. Hertz, H. Über die Berührung fester elastischer Körper. Journal für die reine und ange wandte Mathematik 92 (1982) 156-171.
21. Ruiz, C., Boddington, P. H. B., Chen, K. C. An investigation of fatigue and fretting in a dovetail joint. Experimental Mechanics 24 (1984) 208-217.
22. ABAQUS/Standard User's Manual, Version 6.14.
23. Vázquez, J., Erena, D., Navarro, C., Domínguez, J. 3D contact effects in fretting fatigue tests. Theoretical and Applied Fracture Mechanics 118 (2020) 103260.
24. Kim, H. S., Mall, S., Ghoshal, A. Two-dimensional and three-dimensional finite element analysis of finite contact width on fretting fatigue. Materials Transactions (2011) 1012201243-1012201243.
25. Namjoshi, S. A., Jain, V. K., Mall, S. Effects of shot-peening on fretting-fatigue behavior of Ti-6Al-4V. Journal of Engineering Materials and Technology 124 (2002) 222-228.
26. Hojjati-Talemi, R., Wahab, M. A., De Pauw, J., De Baets, P. Prediction of fretting fatigue crack initiation and propagation lifetime for cylindrical contact configuration. Tribology International 76 (2014) 73-91.
27. Hojjati-Talemi, R., Wahab, M. A. Fretting fatigue crack initiation lifetime predictor tool: Using damage mechanics approach. Tribology International 60 (2013) 176-186.
28. Hills, D. A and Nowell, D. Mechanics of fretting fatigue. Solid mechanics and its applications 30 (1994).